EXPERIMENTAL EVALUATION OF AIR INJECTION FOR ACTUATION OF ROTATING STALL IN A LOW SPEED, AXIAL FAN

Asif Khalak
Department of Mechanical and Aerospace Engineering
Cornell University
Ithaca, NY

Richard M. Murray
Division of Engineering and Applied Science
California Institute of Technology
Pasadena, CA

ABSTRACT

This paper presents an experimental investigation of the effects of air injection on the rotating stall instability in a low speed axial compressor. Two experiments concerning air injection were tried. The first experiment used a continuous forcing perpendicular to the flow in the same or opposite direction of the tip velocity. The results show a dramatic difference between the two directions, with opposite direction forcing causing a significant increase in performance, and same direction forcing causing a significant decrease in performance. This result contradicts the Emmons stall propagation model. The second experiment investigated the differences with respect to different frequencies of air injection, with the injector pointed at the fan, parallel to the flow. We found that the change in the compressor characteristic in the unstalled region was highly dependent upon the forcing frequency with the maximum change occurring near the frequency of stall.

1 Introduction

Modern gas turbine engines are extremely advanced and complicated systems whose design has evolved over many years. As engines become more advanced, the role of full authority digital engine controllers (FADECs) is becoming increasingly significant in the overall operation and performance of the engine. Currently, digital engine control is primarily at the supervisory level, allowing parameters to be modified quasistatically in response to slowly changing operating conditions. Improved sensing, actuation, and computation have spurred research into more dynamic control of engine systems and in particular active control of compressor instabilities.

Two of the limiting factors in the performance of high performance compressors are rotating stall and surge. Rotating stall refers to a dynamic instability that occurs when a nonaxisymmetric flow pattern develops in the blades of a compressor stage and forces a drastic reduction in the performance of the compressor. This degradation in performance is usually unacceptable and must be avoided. Surge is a large amplitude, axisymmetric oscillation in the compressor which results from exciting unstable dynamics in the overall pumping system. While surge and stall are separate phenomenon, the presence of stall is often a precursor to the onset of surge in many compressor systems.

Ongoing work at Caltech is investigating the use of air injection for nonlinear control of rotating stall and surge in axial flow compressors. The eventual goal is to synthesize practical, nonlinear controllers for active control of propulsion systems. This includes not only the basic stability issues in axial flow compressors, but also disturbance rejection and transient performance problems. As an initial step in this direction, this work presents an experimental study of the forced response of a low speed, axial compressor system using injected air as the actuation mechanism. The compressor system consists of a nozzle, inlet duct, a single stage compressor without inlet guide vanes, an exit duct, and a throttle.

Several researchers have explored techniques for flow actuation. A good overview of the theoretical aspects of flow actuation in the context of rotating stall is found in Hendricks and Gysling (1994). Among those discussed are intake and outlet valves actuators, inlet guide vane actuation, and air jet injection actuation.

The two schemes which have been actually implemented are rotating stall control using inlet guide vanes (IGV) actuation and air injection actuation. The first of these two, actuation of the IGVs, was performed by Paduano et al. (1993). This is based on commanding the angle of the IGVs using servo motors. These IGVs are normally present and of fixed angle in many compressor applications. Air injection was implemented by Day (1993). This used the same control scheme as Paduano, but using an array of 12 circumferentially spaced air injectors. Day also studied the effects of uniform, dynamic injection.

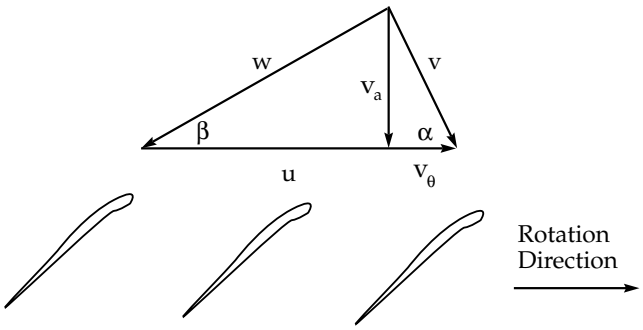

Figure 1: Linear blade cascade. For impellers with high hub to tip ratios, the flow field can be "unwrapped" circumferentially as a good approximation. The variables u and v_a denote tip speed and axial velocity, respectively.

We depart from these previous studies in the sense that we attempt to characterize the use of a single pulsed injector, which provides a non-symmetric view of actuating the flow. Thus, we do not have the option to implement a modal damping scheme.[1]

2 Elements of Rotating Stall Theory

The literature on the theoretical basis of rotating stall is rich and we do not attempt to completely describe it. We discuss only the fundamentals of the theory here. For details concerning the development of the rotating stall models, see, for example, the work of Moore and Greitzer (1984; 1986) and Badmus, Eveker, and Nett (1992).

Works such as Emmons et al. (1955), Marble (1955), and Stenning et al. (1956) lay the foundations for the more sophisticated Moore-Greitzer disturbance model and are of historical interest. These earlier stall models attributed rotating stall to an observable *stall cell*, or low pressure "pocket" which rotates about the compressor face, hence the name *rotating* stall. This description of rotating stall uses a linear cascade to explain stall propagation, but as the results of this work indicate, has somewhat limited predictive value.

These earlier works tackle rotating stall heuristically. We summarize the rationale behind this model as follows, using the nomenclature from Figure 1 in the rotating reference frame of the impeller. As the axial fluid velocity, v_a, decreases relative to the tip speed, u, the angle between $v_a - u$ and the compressor face, called β, decreases. The angle of attack is defined as the blade angle minus the angle of incidence, β. When β decreases, the angle of attack eventually becomes too high. Then the compressor blade stalls in much the same fashion as an airplane wing stalls when it flies at an excessively high angle of attack.

[1] In more recent work, we have modified the rig to include three equally spaced air injectors which can be controlled in a approximately modal fashion.

Stall on the compressor blade creates a low pressure wake where the boundary layer has separated. In turn, the wake diverts the incoming flow to the surrounding blades, effectively increasing the angle of attack for the blade on the left and decreasing the angle of attack for the blade on the right. As a result, the stall cell propagates in the direction opposite of the tip speed. However, when we translate back to a fixed frame, we observe a propagation in the same direction of the impeller rotation (but at a lesser speed than the impeller to account for the stall propagation).

The Moore rotating stall model (Moore, 1984) tries to more explicitly describe the interaction between the compressor and the flow field during rotating stall. In the Moore model, the disturbance pattern in the compressor (i.e. the stall) is assumed axial as well as periodic with respect to stall cells. It is also assumed that for a given rotating frame of reference, the disturbance pattern is quasi-steady. Conditions of the rest of the model which allow solutions of these circumferential disturbances are considered to lead to rotating stall. In other words, rotating stall occurs for a certain set of eigensolutions of the system equations when they produce rotating stall like behavior.

In the model's construction, incompressible flow is assumed throughout. In the upstream region, the flow is assumed to be potential flow, meaning that the unsteady flow will satisfy Laplace's equation. In the downstream region, the possibility of some vorticity entering the system is allowed. The inlet guide vanes (IGVs) are assumed to be axial at entrance and have a discharge angle equal to the outlet guide vanes (OGVs) entrance angle. For both IGVs and OGVs, hysteresis terms (time lags) are included in modeling and the pressure loss at the entrance considered. Rotor blade rows in the compressor are assumed to be separated by stators, and the flow field of a rotor-stator are assumed to be symmetric. The model also assumes that there is no flow development between rows of stator blades or rotor blades.

The results of the model include a theoretical propagation speed for rotating stall given the system parameters and measured lag parameters. In collaboration with Greitzer, who had previously modeled surge (Greitzer, 1976), a later combined disturbance model (Greitzer and Moore, 1986) was developed, usually called the Moore-Greitzer model, which relaxes the previous assumption that the disturbance is quasi-static in some rotating reference frame. The Moore-Greitzer model, then, can address combinations of surge and rotating stall.

Several more complicated models have been proposed in the literature to allow for more complete descriptions of the dynamics in a manner which is still amenable to nonlinear controller design. For a recent survey see (Mansoux et al., 1994) and (Badmus et al., 1992).

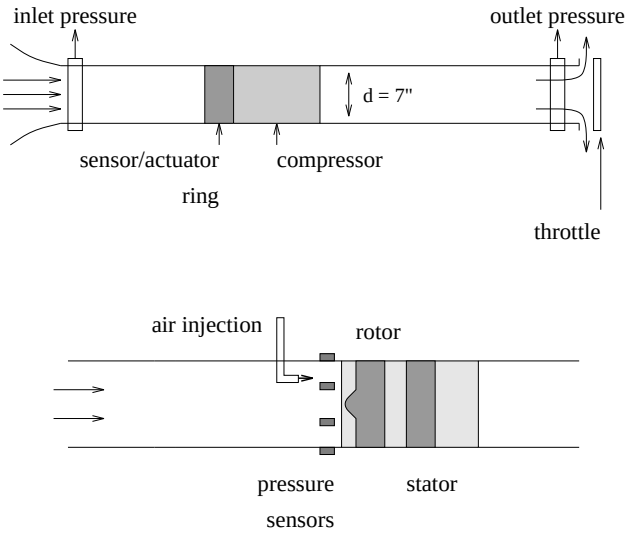

Figure 2: Diagram of experimental setup.

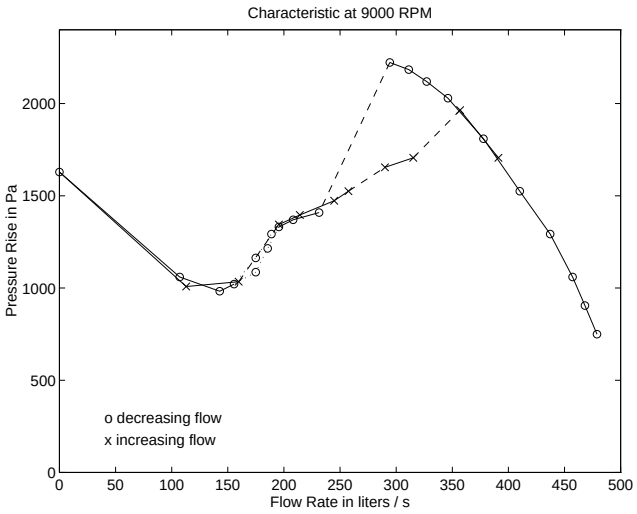

Figure 3: Fan characteristic for Able 29680 compressor at 9000 RPM. Solid lines indicate continuous changes in the operating point and dashed lines represent discontinuous changes in the operating point.

3 Experimental Apparatus

3.1 Compressor system

The Caltech experimental compressor rig is built around an Able 29680 compressor, a small compressor which is normally used to cool the avionics in an MD-11 aircraft. The design operating point for the compressor (at 12000 RPM) gives approximately 4000 Pa (16 in wg) of pressure across the compressor at 425 liters/sec (900 cfm). The fan is powered by a three phase electric motor attached to a variable frequency power converter. By varying the frequency and input voltage of the motor, it is possible to run the compressor at different operating points.

The full experimental setup is shown in Figure 2 and was designed and constructed in accordance with AMCA/ASHRE standards for measurement and calibration of compressors of this type. In addition to the compressor unit, it consists of an inlet nozzle, adjustable downstream throttle, and an optional plenum. Sensors include a pair of static pressure rings on the inlet and outlet sides, a pitot measuring plane near the outlet, and a set of static pressure transducers located in front of the compressor face. Actuation is achieved with a manually operated throttle at the outlet and a single air injector just upstream of the rotor (described in the next subsection).

The static pressure sensors in front of the compressor face are used to measure the pressure variations which are present during rotating stall. There are currently three sensors equally spaced around the outside wall of the compressor inlet. The sensors have a bandwidth of approximately 10 kHz and a resolution of 0.14 Pa (2×10^{-5} psi).

The sensors are interfaced to a data acquisition system via a set of programmable filters. The filters can implement a 4th order Bessel filter at any frequency in the range of 20 Hz to 10 KHz and provide a gain of up to 40 db. The filtered data is a captured by an A/D converter on a 80486-based computer. The computer uses a real-time control package developed at Caltech to capture the data at a programmable sample rate. This control package is currently being used only to read the sensors, but is designed to be used in a closed-loop, real-time control environment. Servo rates of up to 2000 Hz are easily obtained with this system.

Initial experiments on the rig have verified that the compressor system exhibits rotating stall and surge. The measured compressor characteristic is shown in Figure 3. This map gives the steady state relationship between the volumetric flow through the compressor and the pressure across the compressor. The solid lines indicate continuous changes in operating points and the dashed lines indicate discontinuous changes in operating point.

The effect of rotating stall is clearly seen in the measured compressor characteristic. If the flow is decreased beyond the value at which the characteristic reaches its peak, the compressor enters rotating stall and operates an a much lower average pressure. Once in rotating stall the flow must be increased substantially before the system returns to the desired portion of the compressor characteristic.

A sample plot of the inception of stall is shown in Figure 4. Note that the time trace shows no evidence of a modal precursor in the raw data. A power spectral analysis similarly showed no evidence of a modal precursor at incipient stall (at the peak of the characteristic curve). The raw sensor data depicted in Figure 4 was filtered at approximately 300 Hz before being sampled by the computer. For a fan rotational speed of 6000 rpm (100 Hz), the stall cell rotational speed (relative to an inertial frame) is at approximately 4000 rpm (66 Hz). With a 1.8 m^3 (64 cu. ft.) plenum attached, the compressor surges with a surge frequency of approxi-

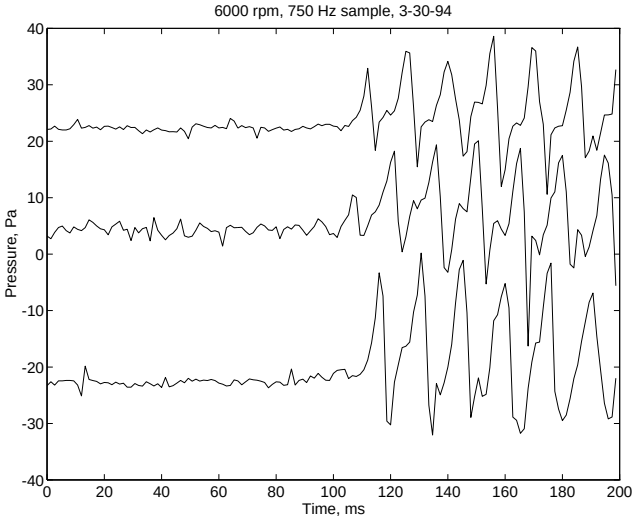

Figure 4: Static pressure sensor data during transition to stall. The top and bottom channels have been offset to separate out the graphs.

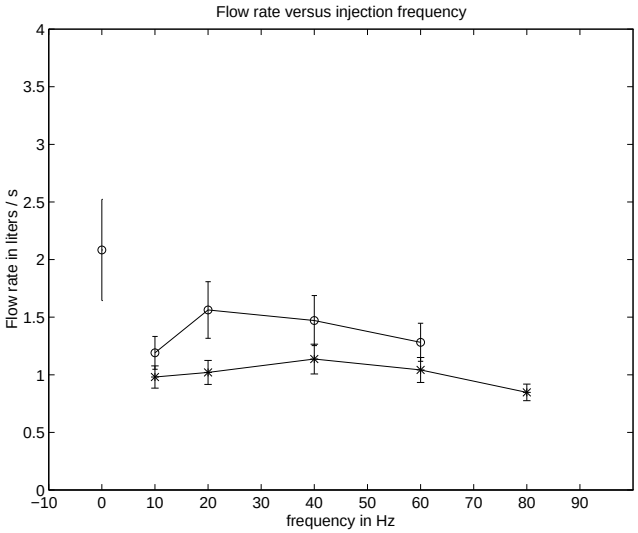

Figure 5: Plot of injector flow rate versus frequency. The o's are for a back pressure of 80 psi x's for 60 psi. Zero frequency point represents continuous flow.

mately 1.7 Hz. This latter value agrees very closely with the Helmholtz resonator frequency determined by treating the air in the inlet and outlet pipes as incompressible and the air in the plenum as stationary.

3.2 Injection System

The injector is a natural gas fuel injector made by ServoJet Products and designed for use in a General Motors research engine. We connected a line with 80 psi of pressure to the injector. The design back pressure is 50-150 psi; below this, air leakage becomes a problem.

The injector port is designed to inject this flow axially, but can be rotated about a radial axis to give a circumferential component to the flow. The air passes through a thin tube 4.125 mm (3/16 inch) in diameter. For the experiments described in this paper, the jet from the air injector was positioned to strike the compressor blades at mid-span and the opening of the injector was approximately 2.5 cm from the rotor face.

The power to the injector is switched on and off by a transistor, which takes its command signal from a frequency generator. Since the frequency generator is adjusted manually, the information from the pressure sensors is not in a closed loop with the actuator yet. This is, however, adequate for the characterization of the actuation.

4 Results

The methods of quasi-static and dynamic measurement described in the previous chapters were used to determine the effect of injecting high pressure air from the injector just described. We studied the effect of changing the orientation of the injection as well as the effect of changing the frequency of injection. Throughout the experiments involving the use of air injection, we used a fan speed of 4800 rpm and a back pressure of 80 psi for the injector.

4.1 Injector Flow Rate

For active control to be viable, the air injection must change the flow dynamics at the impeller. To verify that the changes associated with air injection were changes in the way the fan operated, we needed to make sure that the total amount of flow passing through the duct was not significantly affected. The results of this flow rate measurement is shown in Figure 5.

The flow rate measurement was based on the time in which the injector was able to release five liters of air into a inverted bottle, initially filled with water. This is subject to human timing error, which we estimated to be 0.25 seconds. The error bars on Figure 5 are based on this estimate.

The flow rate from the injectors with continuous flow and at 80 psi is 4.4 cubic feet per minute. For a fan speed of 4800 rpm the flow rate at rotating stall was 300 cubic feet per minute, so the injector flow rate is about 1.5% of the total flow for this speed (for periodic injection).

The momentum addition to the fan is significant. Periodic forcing entails a momentum addition of 8% of the mean flow, and continuous injection adds 20% of the momentum of the mean flow. However, we are attempting to actuate the system, thus a momentum addition is necessary. It is important, however, that the flow rate is low. Otherwise there would be an ambiguity in the operating point. The momentum deficit caused by the drag caused by the injection tube is less than 1% of the mean flow.

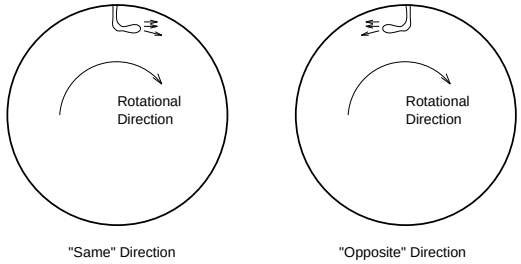

Figure 6: Difference between blowing in the same versus opposite directions. View facing the compressor (flow into page).

4.2 Effect of Injector Orientation

The orientation of the injection is a major influence on the quasi-static fan characteristic, especially near stall. Consider two extreme cases: blowing air in the same direction as the tip velocity, and blowing air in the opposite direction (see Figure 6). We term these "opposite direction" injection and "same direction" injection, both referenced to the fan tip velocity. This will effectively place a swirl (i.e. circumferential) component on the inlet flow for the same injection case and a counter-swirl for the opposite injection case.

One might predict, a priori, that a swirl component to the flow in the same direction would effectively reduce the fan speed relative to the flow (the fan still rotates at constant speed with respect to the fixed frame), causing the angle of attack to decrease and delay stall, based on the Emmons model. Along the same lines of reasoning, blowing in the opposite direction would make stall more imminent. However, for the experiments presented here, the conclusions based on this reasoning are incorrect. In fact, the results are the reverse of what one expects from the aforementioned reasoning.

The results in Figure 7 show the quasi-static fan characteristic with injection in the same and the opposite direction of the fan tip velocity. These are digitally filtered representations of unsteady data, with the high frequency components thrown away. Each case is compared to the characteristic with no injection. We see that in the case of injection in the opposite direction of the fan tip velocity, the point of stall inception is at a flow rate almost 10% less than with no injection at all, and the head rise is increased about 10%. The injection in the same direction, however, stalls at a head rise of more than 15% less than the unforced characteristic. The flow rate becomes greater in the same direction injection case but not significantly compared to the injection flow rate.

A slight digression regarding the filtering of the data is in order. Since the compressor characteristic is discontinuous, it is not appropriate to filter the entire set, because this attempts to round out the discontinuity. Thus, the data was filtered in two sets, pre-stall and post-stall and then patched back together.

Apart from simply the change in the stall point, there are

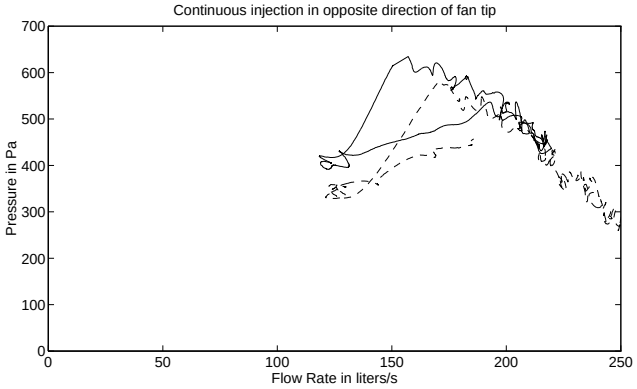

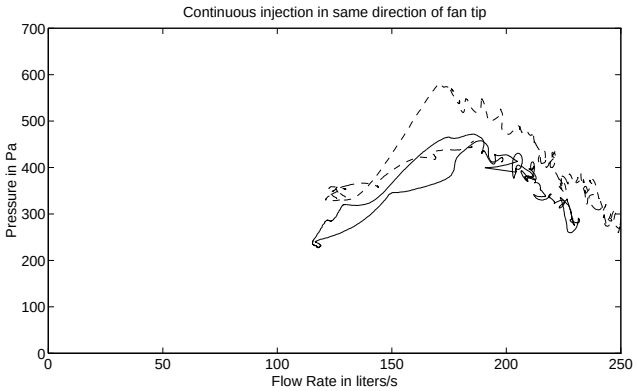

Figure 7: Injector pointed transverse to flow, either in same or opposite direction of impeller tip. The dashed lines show the unforced compressor characteristic.

other changes in the shape of the characteristic, especially in the case of injection in the same direction. Specifically, the air injection in the same direction causes the slope discontinuity associated with stall to be less severe than in the unforced case or the case of injection in the opposite direction.

We notice that the characteristic with opposite direction injection lies above the unforced characteristic. The unstalled segment in the opposite direction case is parallel to the unforced case, as is the stalled segment. However, the head rise is substantially higher in the stalled section of the curve, while it is not in the unstalled section. These trends carry over to the effects of straight injection (into the fan) at varying frequencies.

Because of the change in the shape of the characteristic in the same direction case, the comparison to the unforced characteristic is not so applicable. One element that does carry over (as we would expect) is that the characteristic in the normal operating regime is parallel to the unforced case.

These facts still do not address the question of why the characteristic should change as a result of forcing in this way and why the reasoning outlined at the beginning of this sec-

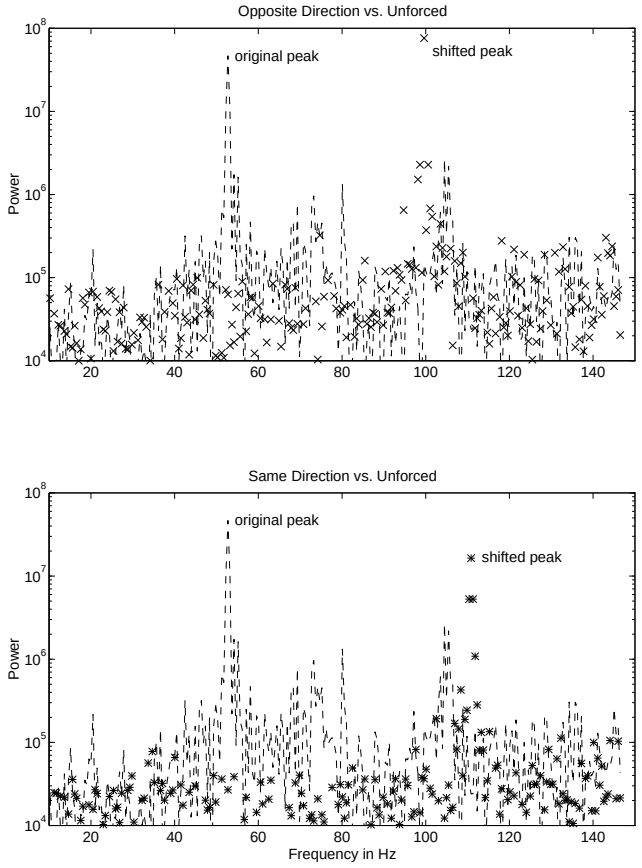

Figure 8: Power spectra comparison of no injection, injection in the same direction as the tip velocity and injection in the opposite direction. The no injection case is dashed, the same direction case is represented by `*`'s and the opposite direction case is represented by `x`'s.

tion is faulty. Assuming that the injector does place an inlet swirl on the flow, which effectively speeds up or slows down (relative to the flow) the fan depending on the direction the injector is placed, this does explain the shift in the quasi-static characteristic. For injection in the same direction, we expect a reduction in head for a given flow rate in the normal operating regime, and for injection in the opposite direction we expect the opposite. This is heuristically true for the unstalled segments of the characteristic. However, it does not, as we mentioned before, explain the behavior near the stall region.

Unsteady pressure measurements can tell us more about the influence of transverse injection on the dynamics of rotating stall. A comparison of the power spectra in the stalled operating regime of an unforced, opposite direction injection, and same direction injection is shown in Figure 8.

Two features are readily apparent upon inspection of the

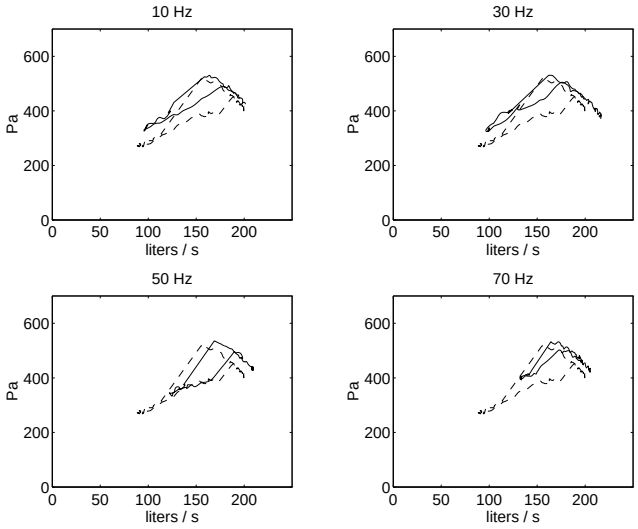

Figure 9: Fan characteristics for various injection frequencies. Unforced characteristic (head rise vs. flow rate) is shown dashed, compared to solid, actuated characteristic.

graph. First, the injection (in both cases) causes a shift in the power spectra from the first harmonic to the second harmonic. One could say that this involves a shift from first mode rotating stall to second mode.

The second feature is that while injection in the same direction increases the frequency of the harmonic peak, injection in the opposite direction decreases the frequency of the harmonic peak. Note that the direction of the tip velocity is also the same direction as the stall oscillation. This feature holds for both first and second mode for both the first and second harmonic, but is more prominent for the second harmonic of rotating stall.

We may then deduce that the air injection is indeed changing the *dynamics* of the problem. In some sense, injecting the air in the opposite direction of the rotating stall wave "slows" it, while injecting air in the same direction of the stall wave "accelerates" it. That is, the characteristic frequencies lessen for opposite direction injection and increase for same direction injection.

4.3 Effect of Injector Forcing Frequency

Apart from the effect of injection at different angles, we also investigated the effect of injecting parallel to the flow, but at different frequencies of forcing (i.e. injection). The results of this investigation are encapsulated in Figure 9 which shows the fan characteristics of several injection frequencies, each compared with the unforced fan characteristic.

On the unstalled branch of the characteristic, the 10 Hz injection is close to the same as the unforced fan, but with a slightly higher flow rate. This widens so the flow rate increase is more significant between unforced and 30 Hz. At 50 Hz, the gap between flow rates for the same head rise is

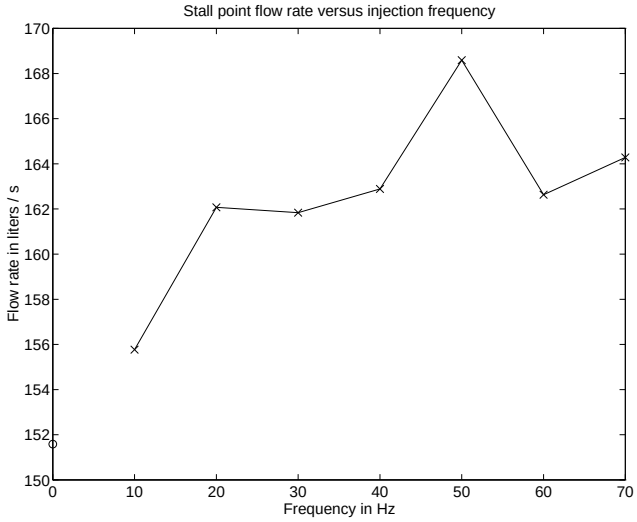

Figure 10: Flow rate of the onset of rotating stall versus injection frequency. The "o" at 0 Hz represents the flow rate of the unforced fan.

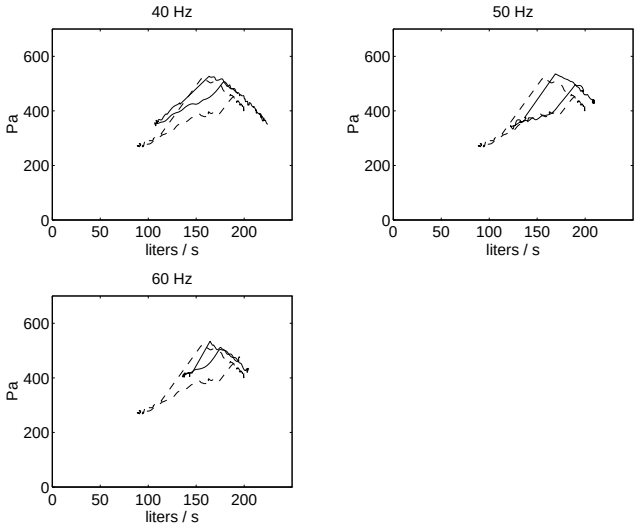

Figure 11: Fan characteristics for frequencies near 50 Hz. Unforced characteristic (head rise vs. flow rate) is shown dashed, compared to solid, actuated characteristic.

largest, at 15% of total flow. This gap decreases for 70 Hz.

The stall inception point moves accordingly. The difference between the forced and unforced head rise is relatively constant with respect to frequency, but the flow rate at stall inception changes dramatically depending upon the frequency. This is shown in Figure 10. Clearly, there is a peak at 50 Hz in the flow rate at incipient stall. Interestingly enough, the stall frequency for the compressor at this speed (4800 rpm) is 52 Hz, as shown in Figure 8.

There are also some interesting features associated with the stalled branch of the characteristic. For all the frequencies except for 50 Hz on Figure 9, the stalled branch of the compressor is on a branch higher than the unforced characteristic and parallel to it. For 50 Hz, however, the stalled branches of the characteristic converge for unforced and forced conditions at the 50 Hz stall frequency.

Clearly, there are great changes near 50 Hz. The characteristics of the frequencies near 50 Hz are compared in Figure 11. We can see that the hysteresis becomes bigger from 40 Hz to 50 Hz, but is reduced from 50 Hz to 60 Hz. The stalled portion of the characteristic for 60 Hz forcing seems to be the same line as in 40 Hz, but the segment in the 60 Hz line is much shorter and of higher flow rate. The hysteresis for this case, as well as 70 Hz in Figure 9 is substantially lower than that for 50 Hz or less.

An interesting quantity related to the hysteresis is the difference between the flow rate at imminent "unstall," i.e. the point at which the operating point goes back to the normal branch, and imminent stall. For the unforced case, this difference is positive. It continues to be positive for low frequencies, looks to be approximately zero for frequencies near the stall point, and is negative for 70 Hz. Thus, we see a monotonically decreasing trend between this difference and forcing frequency.

Looking at the unsteady pressure during stall gives the result that the peak amplitude in the power spectrum moves from the stall frequency to the forcing frequency. In the case of forcing at 50 Hz, however, these frequencies coincided. This may explain the fact that the stalled branch of the 50 Hz characteristic corresponds to the stalled branch of the unforced fan.

To recapitulate, with straight injection, the characteristic has a greater head rise than the unforced characteristic for all frequencies in the unstalled region. Among different frequencies, the gap peaks near the stall frequency of 52 Hz. Also, near the stall frequency at 50 Hz, the stalled branch of the characteristic reattaches onto the unforced characteristic. Finally, the amount of hysteresis, measured by the difference between stalled and unstalled flow rates decreases with increasing injection frequency.

5 Summary and Discussion

Air injection actuation has been studied in the context of its effects on the rotating stall instability in an axial compressor. The steps leading to the investigation of air injection included the design and construction of an axial fan rig. This rig has the facility for acquiring steady pressure information at locations upstream and downstream of the fan, and for acquiring unsteady pressure information at the impeller face. Our actuator setup is unique from those studied in the literature (Paduano (1993), and Day (1993)) in that we consider the effect of a single actuator. Both Paduano and Day use an array of equally spaced actuators in an effort to delay the onset of rotating stall.

The first experiment tried with the injector was a continuous forcing perpendicular to the flow in the same or

opposite direction of the tip velocity. The puts a swirl or counter-swirl component on the flow, respectively. The results show a dramatic difference between the two directions with opposite direction forcing causing a significant increase in performance and same direction forcing causing a significant decrease in performance. The changes are all several times greater than the increased air flow from the injector, which is about 1.5% of the total air flow. These results have not been previously observed in the literature.

The results from the first experiment are not well explained by the Emmons (1955) picture of rotating stall. In fact, predictions based on the Emmons picture give the opposite answer to the results observed. This implies that a simplistic view of rotating stall, by analogy to a linear cascade ignores the fundamentals of the problem. One explanation is that in our particular setup, the stator may stall before the rotor. Thus, a counter swirl would still increase the performance because the increase in the rotor performance would be more than the decrease associated with the stator stall. A pre-swirl, however, would simply degrade the performance of the rotor.

The second experiment investigated the differences with respect to different frequencies of air injection, with the injector pointed at the fan, parallel to the flow. We found that the change in the compressor characteristic in the unstalled region was highly dependent upon the forcing frequency with the maximum change occurring near the frequency of stall. Changes in the stalled characteristic of the compressor were, however, minimal near the frequency of stall and significant elsewhere. These results, as well, have not been previously documented.

Current work on the system by other researchers at Caltech has made use of the results presented here to develop active control methods for rotating stall. In particular, it appears that inducing input swirl plays a significant role in the effectiveness of air injection for stabilizing stall on our rig. By carefully controlling when the air jet is turned on, we are able to get stable operation slightly beyond the normal operating point of the compressor and, perhaps more importantly, eliminate the hysteresis loop in the compressor characteristic. These results will be the subject of future publications.

Acknowledgements

The authors would like to acknowledge Gavin Hendricks for his suggestion regarding the difference between same and opposite direction forcing. We would also like to thank Professor Allan Acosta, Raff D'Andrea, Wayne Hurwitz, and Donald North for their help in this research effort.

References

Badmus, O. O., Eveker, K. M., and Nett, C. N., 1992, Control-oriented high-frequency turbomachinery modeling: Theoretical foundations. In *28th Joint Propulsion Conference*. AIAA Paper No. 92-3314.

Day, I. J., 1993, Active suppression of rotating stall and surge in axial compressors. *ASME Journal of Turbomachinery*, vol. 115, 40–47.

Emmons, H. W., Pearson, C. E., and Grant, H. P., 1955, Compressor surge and stall propagation. *ASME Transactions*, vol. 6, 429–455.

Greitzer, E. M., 1976, Surge and rotating stall in axial flow compressors: Part 1—theoretical compression system model, Part 2—experimental results and comparison with theory. *ASME Journal for Engineering for Power*, vol. 98, 190–198.

Greitzer, E. M. and Moore, F. K., 1986, A theory of post-stall transients in axial compression systems: Part 1—development of equations, Part 2—application. *ASME Journal for Engineering for Power*, vol. 108, 68–78, 231–239.

Hendricks, G. J. and Gysling, D. L., 1994, Theoretical study of sensor-actuator schemes for rotating stall control. *AIAA Journal of Propulsion and Power*, vol. 10, 101–109.

Mansoux, C. A., Setiawan, J. D., Gysling, D. L., and Paduano, J. D., 1994, Distributed nonlinear modeling and stability analysis of axial compressor stall and surge. In *American Control Conference*.

Marble, F. E., 1955, Propagation of stall in a compressor blade row. *Journal of the Aeronautical Sciences*, vol. 22, 541–554.

Moore, F. K., 1984, A theory of rotating stall of multistage axial compressors: Parts 1–3. *ASME Journal of Engineering for Gas Turbines and Power*, vol. 106, 313–326.

Paduano, J. D., Epstein, A. H., Valavani, L., Longley, J., Greitzer, E. M., and Guenette, G. R., 1993, Active control of rotating stall in a low-speed axial compressor. *ASME Journal of Turbomachinery*, vol. 115, 48–56.

Stenning, A. H., Kreibel, A. R., and Montgomery, S. R., 1956, Stall propagation in axial-flow compressors. Technical Report 3580, NACA.